

## High-Energy Phonon Branches of an Individual Metallic Carbon Nanotube

J. Maultzsch,<sup>1</sup> S. Reich,<sup>1</sup> U. Schlecht,<sup>2</sup> and C. Thomsen<sup>1</sup>

<sup>1</sup>*Institut für Festkörperphysik, Technische Universität Berlin, Hardenbergstrasse 36, 10623 Berlin, Germany*

<sup>2</sup>*Max-Planck-Institut für Festkörperforschung, Heisenbergstrasse 1, 70569 Stuttgart, Germany*

(Received 13 December 2002; published 19 August 2003)

We present excitation-energy dependent Raman measurements between 2.05 and 2.41 eV on the same individual carbon nanotube. We find a change in the Raman frequencies of both the *D* mode ( $63\text{ cm}^{-1}/\text{eV}$ ) and the high-energy modes. The observed frequencies of the modes at  $\approx 1600\text{ cm}^{-1}$  as a function of laser-energy map the phonon dispersion relation of a metallic tube near the  $\Gamma$  point of the Brillouin zone. Our results prove the entire first-order Raman spectrum in single-wall carbon nanotubes to originate from double-resonant scattering. Moreover, we confirm experimentally the phonon softening in metallic tubes by a Peierls-like mechanism.

DOI: 10.1103/PhysRevLett.91.087402

PACS numbers: 78.30.Na, 63.22.+m, 78.67.Ch

Raman spectroscopy is a simple and yet powerful method to study the structural and electronic properties of carbon nanotubes. The tube diameters are calculated from the frequencies of the radial breathing mode (RBM) [1–3]. If the high-energy mode (HEM) between 1500 and  $1600\text{ cm}^{-1}$  has an explicit Breit-Wigner-Fano profile, it is usually taken as an indication for the metallic character of the tube [4,5]. The defect concentration in the sample is estimated from the intensity ratio of the disorder-induced *D* mode to the HEM or to a second-order mode [6,7]. It was even attempted to determine the chiral indices ( $n_1, n_2$ ) of isolated tubes by combining the information given by the RBM and the HEM [3,8,9].

Despite this extensive use of Raman spectroscopy on carbon nanotubes, the interpretation of the Raman spectra is still subject to controversial discussion involving two conceptually different models based on single-resonance and double-resonance scattering. The applications described above were developed for the more conventional single-resonance model [1–4,8,9], although neither of these effects has yet been verified by independent experimental techniques. The double-resonance model [10,11], on the other hand, leads to different conclusions about the properties of the investigated nanotubes. For example, a small *D*/HEM ratio does not necessarily indicate a low defect concentration, but the presence of semiconducting or metallic  $\mathcal{R} = 1$  tubes [10,12]. The frequency of the RBM is not only determined by the tube diameter, but also by the excitation energy. Furthermore, while so-called metallic Raman spectra originate (as in the single-resonance picture) from only metallic tubes, the so-called semiconducting spectra might come from both semiconducting and metallic tubes. In addition, a double-resonance process in carbon nanotubes would allow the investigation of the phonon dispersion relations by changing the excitation energy, as has been attempted for graphite [13]. An experimental proof as to which model is correct is thus essential for future work on carbon nanotubes.

The unambiguous signature of defect-induced, double-resonant Raman scattering is the laser-energy dependence of the Raman frequencies, since at each laser energy different phonon modes with large wave vectors are selected. On the other hand, as long as the experiments are performed on tube ensembles, i.e., many tubes of different chirality are simultaneously excited, it is difficult to rule out one of the models experimentally. Any dependence of the Raman spectra on excitation energy is in the single-resonance model explained as a result of exciting different tubes when changing laser energy [1]. In contrast, in the double-resonance model this dependence is interpreted as a process originating from each of the excited tubes and, consequently, predicted also for a single, isolated tube. Therefore, the obvious experimental discrimination between the two interpretations is found in laser-energy dependent Raman measurements on one isolated tube.

The Raman experiments on isolated or nearly isolated nanotubes that have been reported so far do not comprise any laser-energy dependent study on the *same* isolated nanotube [8,9,14]. Very recently, Jorio *et al.* [15] presented Raman spectra of the same isolated tube at 2.41 and 2.54 eV, where they did not find any frequency shift. This investigation, however, was performed for only two laser energies less than the phonon energy apart.

In this Letter, we address the current discussion of whether the Raman process in carbon nanotubes is single or double resonant, and hence involves only  $\Gamma$ -point phonon modes or phonons with large wave vectors. We present Raman spectra recorded from the *same* specific isolated (or nearly isolated) nanotube at five different laser wavelengths between 2.05 and 2.41 eV. The *D* mode shifts by about  $63\text{ cm}^{-1}/\text{eV}$ ; at the same time also the HEM changes in shape and frequency significantly with varying laser energy. We show that the frequencies of the HEM as a function of excitation energy can be mapped on the phonon dispersion relation of the excited tube. Our results clearly show the

validity of the double-resonance Raman process for a single tube.

Carbon nanotube samples were prepared from HiPCo-grown tubes with a typical diameter distribution of  $1.05 \pm 0.15$  nm [16,17] on a Si substrate. In Fig. 1 we show an atomic-force microscopy image of a  $6 \times 6 \mu\text{m}^2$  area of our sample. Single tubes or thin bundles consisting of just a few tubes are dispersed on the substrate with an average density of 0.5 tubes per  $\mu\text{m}^2$ . Raman measurements were performed using a microscope on a Dilor XY 800 triple spectrometer equipped with a charge-coupled device. The tubes were excited with a dye laser and an Ar-Kr laser. To avoid damage of the tubes, the laser-power density on the sample was kept below  $40 \mu\text{W}/\mu\text{m}^2$ . The Raman frequencies were calibrated using the emission lines of a neon lamp. We measured the tube (or very thin bundle) indicated in Fig. 1, which could be specified with the help of the electrode marker. By averaging cross sections along the tube axis we obtain a value of 2.8 nm, indicating the presence of probably 2–3 tubes. When the sample was moved by  $0.5\text{--}2 \mu\text{m}$  with respect to the laser spot, the Raman signal vanished. The laser was polarized parallel to the tube axis in order to obtain the maximum Raman signal; in perpendicular polarization the signal disappeared, in agreement with experimental and theoretical work [18–21]. The RBM signal (Fig. 2 left) was very weak in general and overlapped with the second-order acoustic spectrum of Si; above 2.38 eV laser energy we were not able to detect the RBM. Nevertheless, between 2.05 and 2.18 eV we found a weak RBM peak at  $200 \text{ cm}^{-1}$  and a second one at  $249 \text{ cm}^{-1}$  which was slightly upshifted at 2.05 eV. Thus we can safely assume that at each of our five different laser energies the signal came from the same 1–2 tubes. The experiment was repeated on a second spot with similar results.

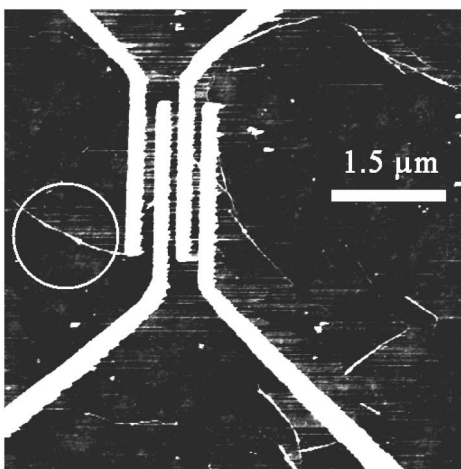


FIG. 1. Atomic-force microscopy image of a  $6 \times 6 \mu\text{m}^2$  area of the sample. Several isolated tubes or very thin bundles are dispersed on the substrate. The white circle indicates the investigated tube close to the four vertical electrodes.

In Fig. 2 we show the Raman spectra of the tube indicated in Fig. 1 excited with laser energies between 2.05 and 2.41 eV. The *D*-mode frequency increases with increasing excitation energy. Clearly, also the two HEM peaks change considerably in frequency and shape. The HEM exhibits a metallic line shape at 2.05 eV; i.e., the peak at  $1550 \text{ cm}^{-1}$  is large in intensity and strongly broadened toward lower frequencies. At higher laser energies the linewidth and intensity decrease; the frequency increases, until the line shape has semiconducting character at 2.38 and 2.41 eV. In Fig. 3 (left) we plotted the peak positions as a function of excitation energy. The frequency of the upper peak first decreases and then increases again, while the frequency of the lower peak on average increases with laser energy. This observation of excitation-energy dependent Raman frequencies in the same nanotube provides clear evidence for the double-resonance process in carbon nanotubes, as we will discuss below in detail.

The double-resonance process, as suggested for the first-order Raman spectra of carbon nanotubes, is a fourth-order process involving elastic scattering of the electrons by defects [22]. This allows, in contrast to the single-resonance model, phonons with large wave vectors to contribute to the scattering. Therefore, the otherwise rather restrictive double-resonance condition [23] can be fulfilled at any laser energy above the fundamental gap. The characteristic of defect-induced, double-resonant scattering is the dependence of the Raman frequencies on excitation energy for an individual tube [11].

In contrast, the single-resonance interpretation assumes that the Raman spectra result from conventional first-order scattering by only  $\Gamma$ -point modes. The term “resonant” is used only if the laser energy matches a singularity in the electronic density of states (DOS).

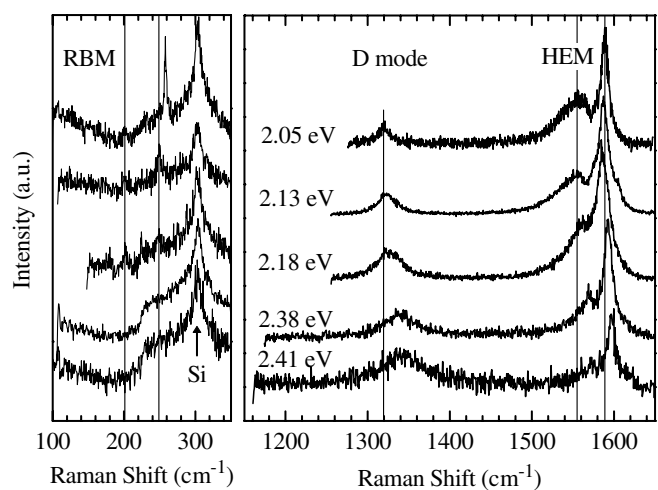


FIG. 2. Raman spectra of the same tube recorded at different laser energies (given next to the spectra). The spectra are scaled to about the same amplitudes and offset vertically. The vertical solid lines indicate the frequencies of the *D* mode and the HEM peaks in the spectrum taken at 2.05 eV.

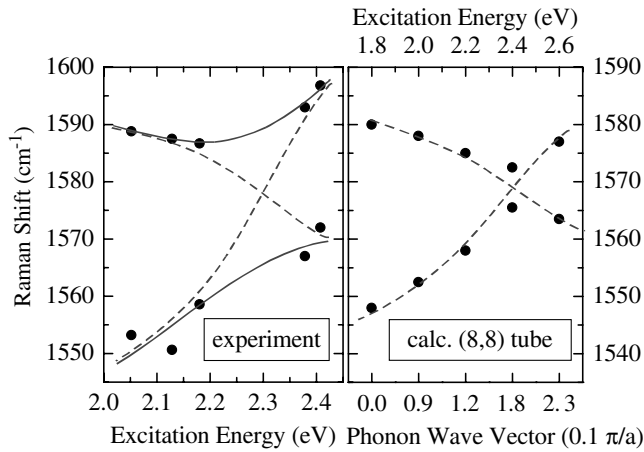


FIG. 3. Left: High-energy mode frequencies as a function of excitation energy. The solid and dashed lines are a guide to the eye to sketch the proposed resemblance of the phonon dispersion relation of a chiral and an achiral metallic tube, respectively. Right: Calculated high-energy phonon frequencies of the (8,8) tube as a function of laser energy (top axis) and of the double-resonant phonon wave vector (bottom axis); dashed line as on the *left*. The relation between laser energy and phonon wave vector is not linear.

According to this model, the Raman frequencies of an individual tube are *independent* of the excitation energy but the Raman signal vanishes with the laser being less resonant with the singularities in the electronic DOS.

In order to understand the different phonon frequencies (Fig. 3, left) within the single-resonance model, one would have to assume that the tube in Fig. 1 comprises five different nanotubes and coincidentally each of the five laser wavelengths selects one of the tubes by exactly matching the singularities in the electronic DOS. This appears unlikely, in particular, in view of the almost constant RBM frequencies. Second, the frequency of the HEM would change according to the dependence of the  $\Gamma$ -point phonon frequencies on the tube diameter. As the optical-phonon frequencies decrease with decreasing tube diameter [24,25], a monotonic downshift of the HEM frequencies with increasing excitation energy is expected. Third, the Raman intensity should not vary significantly. These predictions from the single-resonance model are obviously in disagreement with our experimental results shown in Fig. 3 and the inset to Fig. 4.

To discuss our results following the double-resonance model, we calculated the energies for optical transitions at the singularities in the electronic DOS by the tight-binding approximation including third-nearest neighbors [26]. For the range of diameters and laser energies in our experiments we found the optical transitions of predominantly metallic tubes, most of which are  $\mathcal{R} = 3$  tubes. This is in agreement with the observation of the *D* mode and the prediction of double-resonant *D*-mode scattering only for  $\mathcal{R} = 3$  tubes [10]. Let us therefore assume that in our experiment a particular metallic tube is excited and

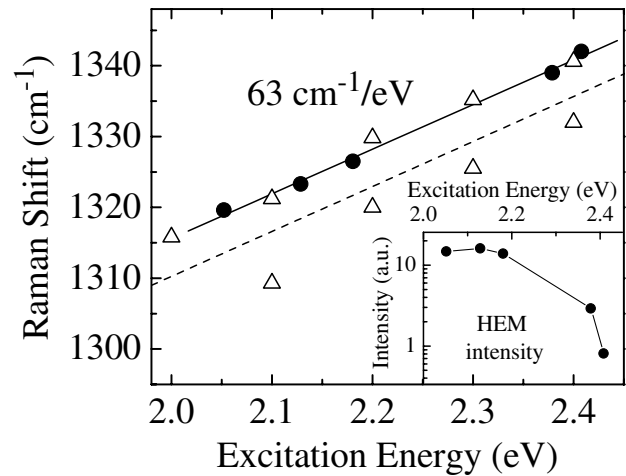


FIG. 4. Experimental *D*-mode frequency as a function of excitation energy (dots) and calculated values for the (8,8) tube (triangles). The solid (dashed) line is a linear fit to the experimental data (theory). Inset: Relative Raman intensity (peak area normalized to laser power, integration time, and spectrometer sensitivity) of the HEM as a function of laser energy.

that the laser energy is in the vicinity of a singularity in the electronic DOS. In this case, the double-resonant phonon wave vectors contributing to the HEM are near the  $\Gamma$  point (but still large compared with the wave vector of light). In metallic tubes the upper phonon branch with band index  $m = 0$  (longitudinal mode in achiral tubes) was proposed to drop below the second  $m = 0$  branch (transversal mode) in a Peierls-like transition [25]. When moving away from the  $\Gamma$  point, this longitudinal branch exhibits a strong overbending up to  $\approx 1600 \text{ cm}^{-1}$ . In achiral tubes, the two optical-phonon branches cross near the  $\Gamma$  point; in chiral tubes, they have the same symmetry, and an anticrossing of the branches occurs. The double-resonant phonon wave vector increases with increasing laser energy as long as the optical transitions take place within the same electronic bands [11]. Following this interpretation, we expect a change in the HEM frequencies, that corresponds to the phonon dispersion relation. A metallic spectrum is then observed at lower excitation energies (with the phonon wave vectors closest to the  $\Gamma$  point); at higher laser energies the spectra appear more semiconductinglike, as seen in Fig. 2. Therefore, the HEM frequencies as a function of laser energy in Fig. 3 (left) map the dispersion relation of the two optical  $m = 0$  phonon branches of a particular metallic tube. This is indicated by the lines; the bands either cross or exhibit an anticrossing, depending on the chirality of the tube.

The intensity of the HEM peaks (inset of Fig. 4) decreases by a factor of  $\approx 10$  with increasing laser energy further supporting our model [11]. As in single resonance, the Raman intensity depends in the double-resonance—among others—on how close the laser energy is to the singularities in the electronic DOS, which is included in the full integration of the Raman cross section. The

difference between the two models is that in single resonance a systematic decrease of intensity implies constant frequencies (exciting the same tube), whereas an intensity decrease in double-resonance occurs simultaneously with a continuous frequency change.

To illustrate our model, we show in Fig. 3 (right) and Fig. 4 the Raman frequencies calculated for an (8,8) tube within the double-resonance [11]. We used a phonon dispersion relation as described in Ref. [24], which we modified to obtain the drop of the longitudinal phonon frequency at the  $\Gamma$  point. The bottom axis in Fig. 3 (right) indicates the average value of the phonon wave vectors contributing to the Raman signal, thus indicating the phonon dispersion. We find an excellent qualitative agreement with the experimental results. Note that the calculated frequencies depend on the chirality and diameter of the tube and on the approximations for the electron and phonon dispersions, thus an exact correspondence of the absolute frequencies is not expected.

The weak metallic shape of the HEM in our spectra is in accordance with a recent explanation by Jiang *et al.* for the metallic spectra, which is based on strong interaction of phonon and plasmon modes [5]. They showed that the metallic line shape is much stronger in nanotube bundles than in isolated tubes. Their model also required large phonon wave vectors, which were *ad hoc* introduced, whereas our interpretation additionally gives a physical reason for the predominance of the non- $\Gamma$  point modes.

Finally, we discuss the laser-dependent shift of the  $D$  mode. Although the *presence* of the  $D$  mode in carbon nanotubes is now widely accepted as being due to a double-resonant process, there is still some discussion as to whether the *shift* and the diameter dependence of the  $D$  mode originate from the double resonance [14,27]. Since so far the  $D$ -mode shift has been observed only in bulk samples, some interpretations implicitly ascribe the frequency shift to a diameter and chirality selective process in inhomogeneous bulk samples [27]. As for the HEM, the single-resonance picture predicts no excitation-energy dependence of the  $D$  mode in an individual tube. In contrast to this prediction, we find an frequency shift of  $63 \pm 2 \text{ cm}^{-1}/\text{eV}$  for our tube (Fig. 4), which is in good agreement with the shift of  $40\text{--}75 \text{ cm}^{-1}/\text{eV}$  predicted by double-resonance theory [10]. Moreover, from the double-resonance model follows the same diameter dependence of the  $D$  mode as reported in Ref. [14], i.e., the  $D$  mode on average increases with increasing diameter [10].

In conclusion, we presented experimental proof of the double-resonance process as the origin of the Raman spectra in carbon nanotubes by excitation-energy dependent Raman measurements on individual nanotubes. As predicted by double-resonance theory, we found that both the  $D$  mode and the HEM frequencies in the first-order Raman spectra depend on excitation energy. The  $D$  mode of the particular tube in our experiments shifted by

$63 \text{ cm}^{-1}/\text{eV}$ ; the HEM frequencies, following the double-resonance model, resemble the optical-phonon branches of a metallic tube near the  $\Gamma$  point.

As a consequence, a “metallic” HEM in the Raman spectra indicates metallic nanotubes in the sample, while a “semiconducting” HEM can originate from both semiconducting and metallic tubes. Moreover, a small intensity of the  $D$  mode can indicate both a low defect concentration in the sample or scattering by semiconducting tubes. Finally, the RBM frequencies should depend on the laser energy as well. The shift is negligible as long as the laser energy is near the singularities in the electronic DOS, but may amount to several wave numbers otherwise. In principle, the double-resonance process allows the experimental determination of the phonon dispersion relations of carbon nanotubes, if the chirality and electronic structure of the investigated tube are known independently. This will remain a challenging task for future work on carbon nanotubes.

We acknowledge useful discussions with M. Burghard. This work was supported by the DFG under Grant No. Th 662/8-1.

- 
- [1] A. M. Rao *et al.*, *Science* **275**, 187 (1997).
  - [2] M. Milnera *et al.*, *Phys. Rev. Lett.* **84**, 1324 (2000).
  - [3] R. R. Bacsa *et al.*, *Phys. Rev. B* **65**, 161404(R) (2002).
  - [4] M. A. Pimenta *et al.*, *Phys. Rev. B* **58**, R16 016 (1998).
  - [5] C. Jiang *et al.*, *Phys. Rev. B* **66**, 161404(R) (2002).
  - [6] L. Zhang *et al.*, *Phys. Rev. B* **65**, 073401 (2002).
  - [7] J. Maultzsch *et al.*, *Appl. Phys. Lett.* **81**, 2647 (2002).
  - [8] Z. Yu and L. E. Brus, *J. Phys. Chem. B* **105**, 6831 (2001).
  - [9] A. Jorio *et al.*, *Phys. Rev. Lett.* **86**, 1118 (2001).
  - [10] J. Maultzsch *et al.*, *Phys. Rev. B* **64**, 121407(R) (2001).
  - [11] J. Maultzsch *et al.*, *Phys. Rev. B* **65**, 233402 (2002).
  - [12]  $\mathcal{R} = 3$  if  $(n_1 - n_2)/3n$  is an integer and  $\mathcal{R} = 1$  otherwise, where  $n$  is the greatest common divisor of  $(n_1, n_2)$ .
  - [13] R. Saito *et al.*, *Phys. Rev. Lett.* **88**, 027401 (2002).
  - [14] A. Souza-Filho *et al.*, *Phys. Rev. B* **67**, 035427 (2003).
  - [15] A. Jorio *et al.*, *Phys. Rev. Lett.* **90**, 107403 (2003).
  - [16] M. J. Bronikowski *et al.*, *J. Vac. Sci. Technol. A* **19**, 1800 (2001).
  - [17] A. Kukovecz *et al.*, *Eur. Phys. J. B* **28**, 223 (2002).
  - [18] G. S. Duesberg *et al.*, *Phys. Rev. Lett.* **85**, 5436 (2000).
  - [19] H. H. Gommans *et al.*, *J. Appl. Phys.* **88**, 2509 (2000).
  - [20] S. Reich *et al.*, *Phys. Rev. B* **63**, R041401 (2001).
  - [21] M. Machón *et al.*, *Phys. Rev. B* **66**, 155410 (2002).
  - [22] R. M. Martin and L. M. Falicov, in *Light Scattering in Solids I: Introductory Concepts*, edited by M. Cardona, Topics in Applied Physics (Springer, Berlin, 1983), Vol. 8, p. 79.
  - [23] F. Cerdeira *et al.*, *Phys. Rev. Lett.* **57**, 3209 (1986).
  - [24] J. Maultzsch *et al.*, *Solid State Commun.* **121**, 471 (2002).
  - [25] O. Dubay *et al.*, *Phys. Rev. Lett.* **88**, 235506 (2002).
  - [26] S. Reich *et al.*, *Phys. Rev. B* **66**, 035412 (2002).
  - [27] J. Kürti *et al.*, *Phys. Rev. B* **65**, 165433 (2002).